Damage Effects of γ-radiation on Lipid Bilayers (*).

G. ERRIU (1), S. ONNIS (1), N. ZUCCA (1), M. CASU (2), A. LAI (2)
C. GIORI (3) and G. SCHIANCHI (3)

(1) *Istituto di Fisica Medica dell'Università - 09125 Cagliari, Italia*
(2) *Dipartimento di Scienze Chimiche dell'Università - 09124 Cagliari, Italia*
(3) *Istituto di Scienze Fisiche dell'Università - 43100 Parma, Italia*

(ricevuto il 12 Novembre 1993; approvato il 29 Novembre 1993)

Summary. — The lipid composition of multi-lamellar vesicles of 1,2-dipalmitoyl-*sn*-glycero-3-phosphorylcholine exposed to ^{137}Cs γ-rays depends on the absorbed dose. In fact, ^{31}P and ^{1}H NMR analysis shows that four new molecular species are formed during the irradiation: *a*) 1-palmitoyl-*sn*-glycero-3-phosphorylcholine, *b*) 2-palmitoyl-*sn*-glycero-3-phosphorylcholine, *c*) glycerophosphorylcholine and *d*) free palmitic acid. Neglecting the species *c*), that is present only at high dose and in very small amount, the behaviour of molar fraction *vs.* dose is sublinear for *a*) and *b*), while for *d*) it is almost linear over all the dose range examined. The molecular and structural damage consequences onto the multi-lamellar vesicles, evidentiated by spin-labelling and DSC techniques, are discussed. It is clearly shown, in particular, that the behaviour of the main transition does not depend on the concentration of the lysolecithins, but rather on that of the free palmitic acid, the role of which had previously been entirely neglected.

PACS 87.50 – Biological effects of radiations.
PACS 61.80 – Radiation damage and other structural irradiation effects.

1. – Introduction.

It is well known that biomembranes consist of a lipid bilayer matrix where enzymes, ion-transport and receptor proteins are localized. The modulation of membrane function by the lipid environment is a phenomenon frequently observed when studying enzyme action or transport processes [1,2]. Here, we describe the effects of ionizing radiation on the lipid matrix of membranes, the experiments being carried out on the so-called multi-lamellar vesicles (MLVs), an experimental model consisting of concentric bilayers separated by aqueous spaces.

The effects of γ-radiation on the lipid molecules of bilayers can be ascribed to two processes. In the first one, the radiolysis of lipid molecules is due to the direct

(*) The authors of this paper have agreed to not receive the proofs for correction.

interaction with γ photons or with secondary electrons. In the second one, lipid molecules are indirectly modified by reacting with free radicals produced by the interaction of γ-rays and secondary electrons with the surrounding water molecules. It is however clear that to evaluate the radiation effects as a simple summation of the direct and indirect ones is an over-simplification. In fact, so as the direct effect is likely to be modified by the presence of water, likewise the indirect effect could be considerably different whether the lipid molecules are arranged in bilayers or not.

All conditions being the same, γ-rays effects at molecular level depend on the kind of lipid molecules constituting the bilayers, in particular whether or not double bonds exist in their acyl chains [3]. In the case of unsaturated lecithins (DAPC), numerous studies [4] have shown that lipid peroxidation occurs through several mechanisms of radical chain reaction. Less attention has been paid in the past to the effects on saturated DAPC [5-7]. But recently [8], by mono- and bidimensional NMR techniques, we could gather detailed information on bilayer-arranged saturated DAPC. Within the explored range of absorbed dose, we demonstrated the formation of four new molecular species; namely: two isomeric lysolecithins (LPC), monocarboxyl acid and glycerophosphorylcholine. Also, we could follow the evolution of the bilayer composition as the absorbed dose increased.

The damage caused to lipid molecules cannot but have consequences onto their organization in bilayers. The first experimental evidence of radiation-induced structural bilayers modifications was obtained by scanning differential calorimetry (DSC) [9, 10]. We observed in fact a progressive change with the dose, of several characteristic parameters of the structural transitions of saturated DAPC bilayers. Experiments using other techniques successively confirmed these results [6, 11]. X-ray diffraction analysis was employed to follow the evolution with the dose of the structure of the single phases [7, 12, 13].

However, so far, attempts to relate the molecular and structural damages [6, 7, 12] turned out to be unsatisfactory. Probably this has been due to poor characterization, both qualitative and quantitative, of the new species created in the bilayers by irradiation.

2. – Materials and methods.

Synthetic 1, 2-dipalmitoyl-*sn*-glycero-3-phosphorylcholine (DPPC), 1-palmitoyl-*sn*-glycero-3-phosphorylcholine (P_1PC) free palmitic acid (FPA), glycerophosphorylcholine (GPC), (^{2}H)chloroform, (^{2}H)methanol and ^2H_2O were purchased from Sigma. Only lipid samples showing no TLC-detectable impurities were used.

For preparing the MLVs, DPPC was dissolved in chloroform. The solvent was removed under nitrogen stream and under vacuum, in succession. ^2H_2O was then added to the lipid and the whole was stirred, for at least 30 min, at a temperature 15 degrees above that of the main transition. The MLVs dispersions so obtained were air saturated and contained lipid in concentrations ranging from 11% to 13% (w/w). A similar procedure was followed for preparing the systems P_1PC-water, FPA-water and GPC-water.

The MLVs dispersions were then hermetically sealed and exposed, at room temperature, to γ-rays from a ^{137}Cs source. A dose rate of $(5.1 \pm 0.3) \cdot 10^{-2}$ Gy s^{-1} was evaluated by using solid-state alanine dosimeters irradiated for 1 hour [14, 15]. The irradiation times were set for the absorbed doses: $D_1 = (22 \pm 1)$ kGy, $D_2 = (44 \pm$

$\pm$ 3) kGy, $D_3 = (66 \pm 4)$ kGy. One sample batch was left unirradiated to serve as blank reference.

The changes in the chemical structure of DPPC, due to the irradiation, were determined by ^{1}H and ^{31}P NMR. 0.5 ml volumes of unirradiated and irradiated MLVs dispersions were lyophilized and dissolved in chloroform-methanol (1:2 v/v). Nitrogen was then let bubble through the liquid. The NMR spectra of the samples were recorded at 30 °C on a Varian VXR-300 spectrometer. The ^{31}P spectra were recorded with broad-band ^{1}H decoupling at pulse intervals of 20 s. The spectral assignment of every resonance was obtained as described in ref. [8].

DSC experiments were performed with a Perkin-Elmer DSC 7 calorimeter. MLVs dispersions having a mass as close as possible to $5 \cdot 10^{-6}$ kg were sealed in aluminum pans. Samples mass was checked both before and after scanning, to make sure no water had been lost. All the DSC curves reported are the result of the subtraction of two curves. The second is the DSC curve obtained with empty pans, both in the sample and reference holders. The first is the curve obtained with MLVs in the sample pan. Each sample underwent several thermal cycles between -45 °C to 70 °C, at a 5 °C min^{-1} scanning rate.

For EPR measurements, spin-label 2, 2, 6, 6-tetramethylpiperidine-1-oxyl (TEMPO) was added to both the previously irradiated MLVs samples and to the non-irradiated ones. The molar ratio of TEMPO to DPPC was 10^{-2}. The EPR spectra were obtained in *X*-band from a Varian E9 spectrometer. Modulation frequency: 100 kHz; modulation amplitude: 0.50 G; microwave power: 5 mW. The central line corresponds to $g = 1.995 \pm 0.001$. Before spectra recording, and with sample temperature stabilized to ± 0.1 °C, enough time was let elapse to make sure that TEMPO distribution between water and lipid phase reached equilibrium.

3. – Results and discussion.

Detailed information about the changes produced by γ-radiation in saturated DAPC molecules was obtained by ^{31}P and ^{1}H NMR [8].

In fig. 1, ^{31}P NMR spectrum of DPPC specimens irradiated at the greatest

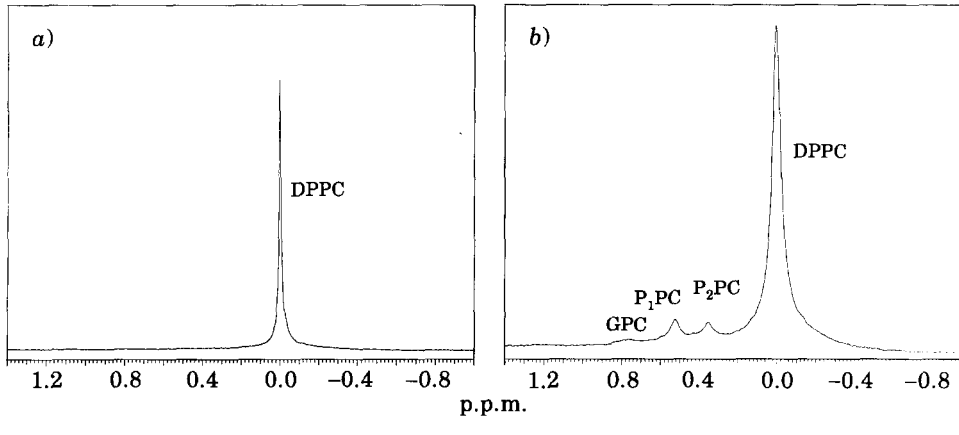

Fig. 1. – ^{31}P NMR spectra of lipids of the MLVs, lyophilized and dissolved in chloroform-methanol (1:2, v/v). *a*) Before irradiation: DPPC only; *b*) at the greatest absorbed dose: mixture of four phosphorylated species.

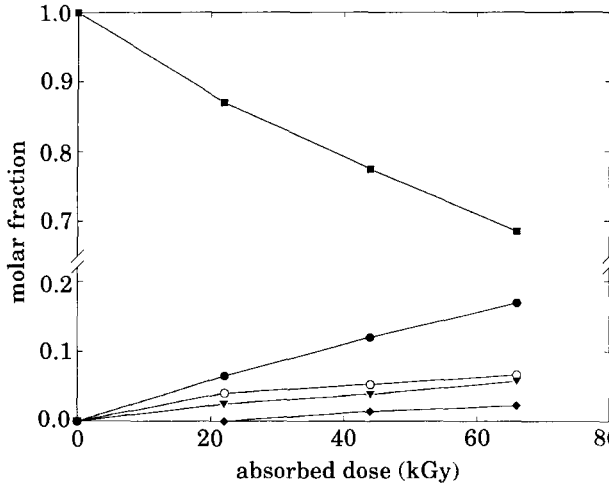

Fig. 2. – Molar fractions of DPPC and relevant degradation products, obtained from ^1H and ^{31}P NMR spectra, at $D_0 = 0$ Gy, $D_1 = (22 \pm 1)$ kGy, $D_2 = (44 \pm 3)$ kGy and $D_3 = (66 \pm 4)$ kGy. ■ DPPC, ○ P_2PC, ▼ P_1PC, ● FPA, ◆ GPC.

absorbed dose is compared with that of an unirradiated specimen. Beyond the signals characteristic of DPPC, those of the following phosphorylated species also show up: P_1PC, its isomer 2-palmitoyl-*sn*-glycero-3-phosphorylcholine (P_2PC), GPC. The molar ratios of the new species to DPPC, measured by the ratios of the respective ^{31}P NMR signal areas, coincide with those from the ^1H NMR signals (spectra not shown). From the latter it is also possible to evaluate the molar ratio of FPA to DPPC, that turns out, as expected, to be consistent with the results relative to the other species simultaneously produced (P_1PC, P_2PC, GPC).

Figure 2 shows how the irradiated-samples composition varies with the absorbed dose. It is evident that, at low doses, the main effect consists of a break of DPPC molecules taking place at one of the two carboxyl groups, which gives origin to formation of P_1PC, P_2PC, FPA. Further irradiation causes another break at the carboxyl group of the LPCs already formed, with production of GPC and further FPA. For P_1PC and P_2PC, the growth of molar fractions *vs.* the dose is sublinear. This is probably due to onsetting of a competition between formation and degradation of the LPCs[8]. As far as the production of FPA is concerned, the two aforesaid mechanisms co-operate, giving rise to nearly linear growth behaviour *vs.* dose.

It is well known that, depending on temperature, the structures of DAPC MLVs in excess water are $L_{\beta'}$, $P_{\beta'}$ and L_α[16-18]. Figure 3*a*) shows the so-called lower transition (LT) and main transition (MT) of unirradiated DPPC MLVs, as they look in DSC curves. As is well known, the LT peak corresponds to $L_{\beta'}$ to $P_{\beta'}$ structure transition, the MT peak to $P_{\beta'}$ to L_α structure transition. The successive figures 3*b*), *c*), *d*) show the DSC curves of irradiated MLVs, the composition of which has been reported above. The dramatic effect of the new molecular species on LT and MT peaks is evident.

However, results of scanning techniques like DSC might depend impredictably on time costants, both of the instrument and of the chemical and physical processes themselves. If, on the contrary, spin-label technique is used, then the mentioned

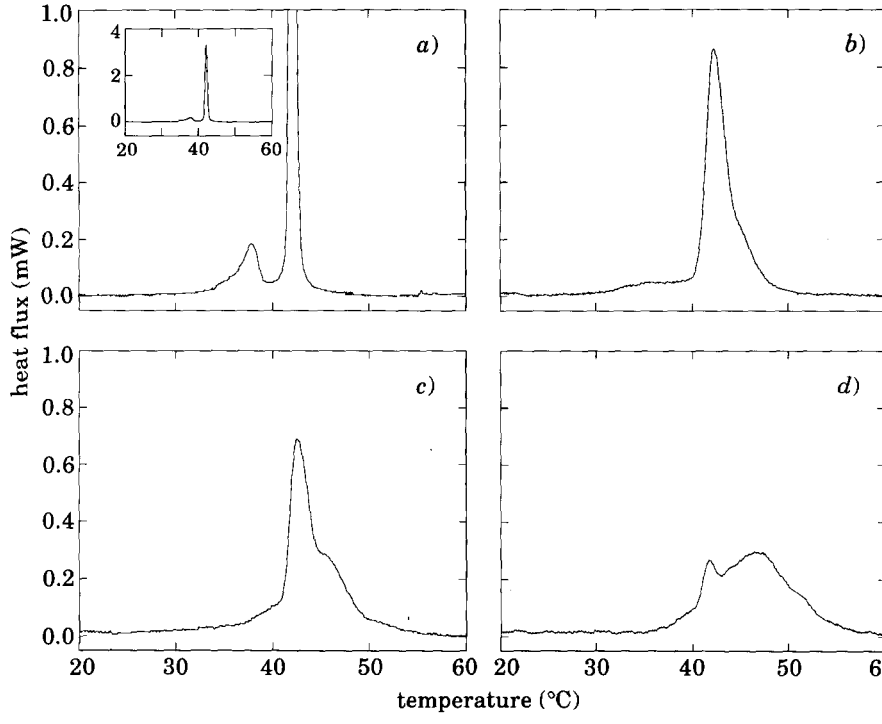

Fig. 3. – DSC curves showing how the new molecular species affect the thermotropic transitions of MLVs. The lipid compositions of the MLVs are those reported in fig. 2, respectively for: *a*) D_0; *b*) D_1; *c*) D_2; *d*) D_3.

drawbacks are entirely avoided, since all the experiment can be carried out in equilibrium condition.

TEMPO spin-label partition between aqueous phase and lipid bilayers of MLVs is known to be sensitive to structural variation of the latter [19-21]. Owing to partition, TEMPO spectrum is the sum of two triplet spectra. The different coupling constants a_H and g-factors for the spin-label in the two phases cause a partial splitting of the corresponding hyperfine lines at high field, even if the components at low or medium field remain unresolved. The high-field line can be decomposed into its two components as follows [22]:

$$S(H_w, H_l, \Gamma_w, \Gamma_l, w_w, w_l) = w_w G(H_w, \Gamma_w) + w_l G(H_l, \Gamma_l), \quad (1)$$

where $G(H, \Gamma)$ stands for the derivative of a Gaussian function, corrected to take into account the superhyperfine splitting due to the ^{13}C; H_w and H_l stand, respectively, for the resonance fields of TEMPO in water and in lipid bilayers; Γ_w and Γ_l are the corresponding peak-to-peak widths; w_w and w_l are the weights of the two components, respectively proportional to the number of spin-label molecules in water ($N_{sp,w}$) and in lipid bilayers ($N_{sp,l}$).

At this point, it is possible to evaluate the parameter f_T, a useful indicator of the

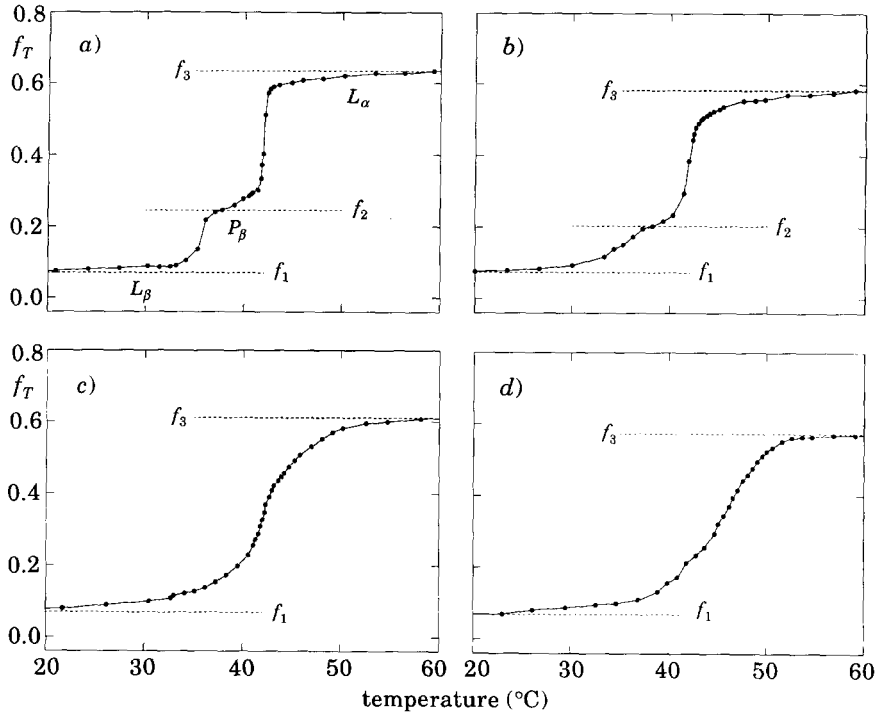

Fig. 4. – Behaviour of the fraction (f_T) of spin-label TEMPO dissolved in the bilayers *vs.* temperature. The f_T values f_1, f_2 and f_3 are assumed to characterize respectively the structures $L_{\beta'}$, $P_{\beta'}$ and L_α of the unirradiated MLVs (or $L_{\beta'}$-like, $P_{\beta'}$-like and L_α-like of irradiated ones). The MLVs compositions are those reported in fig. 2, respectively for: *a*) D_0; *b*) D_1; *c*) D_2; *d*) D_3.

structural transitions [23-26]:

$$f_T = \frac{N_{\mathrm{sp,l}}}{N_{\mathrm{sp,l}} + N_{\mathrm{sp,w}}} = \frac{w_\mathrm{l}}{w_\mathrm{l} + w_\mathrm{w}} . \tag{2}$$

The f_T values reported in the following are the equilibrium values at the indicated temperatures.

For unirradiated DPPC MLVs typical f_T behaviour *vs.* temperature is shown in fig. 4*a*). f_T value can be seen to vary quite slowly except when a structural transition is approached, in agreement with previous results [11,23]. In particular, within the temperature range where the structure is of $L_{\beta'}$ type, the f_T values practically coincide with $f_1 = 0.07$. At the onset of $P_{\beta'}$ structure, f_T value quickly reaches the value $f_2 = 0.25$. Finally, during the next transition to L_α structure, f_T increases further to its final value $f_3 = 0.63$.

The successive figures 4*b*), *c*) and *d*) illustrate the behaviour of f_T for the MLVs irradiated at different doses. It is evident that, irrespective of composition, f_1 and f_3 values are always the same—to within the experimental error—as those of pure MLVs. This fact clearly suggests that the structures developed by the irradiated

MLVs in correspondence of f_1 and f_3 are respectively similar to $L_{\beta'}$ and L_α, for any composition. The transition between these two structures (named in the following $L_{\beta'}$-like and L_α-like) is a direct transition only at high absorbed dose. At low dose (fig. 4*b*)) on the contrary, the presence of an intermediate, $P_{\beta'}$-like structure, is well evident—in agreement with previous diffraction analysis [13]. So that the transitions are still two, say $L_{\beta'}$-like $\rightarrow P_{\beta'}$-like and $P_{\beta'}$-like $\rightarrow L_\alpha$-like.

As can be seen in fig. 3 and 4, both DSC and spin-label techniques show that the structural transitions of irradiated MLVs take place over a whole range of temperature, whose amplitude strongly depends on MLVs composition. Such transitions are clearly not 1st order, in the Ehrenfest sense. On the other hand, neither are «pure» 1st order the structural transitions of bilayers with just one lipid component. Actually, even though such transitions are accompanied by latent heat [16, 27, 28], they also occur over a finite range of temperature—though a rather narrow one [28-30]. According to Ubbelhode analysis [31], these broad transitions can be ascribed to the co-existence of different phases within the same bilayer [28]. The possibility of this co-existence during a transition has been demonstrated by electron microscopy [32, 33].

Now we consider a lipid bilayer originally all in the gel phase. The transition begins at a characteristic temperature, just when small regions of lipid in the liquid-crystalline state begin to form within the bilayer. These regions grow in size as the temperature is further raised, until all of the lipid has reached the liquid-crystalline state. Let us consider a MLVs system at a temperature T within the (diffuse) transition's range. If the corresponding value of the parameter, f_T, is known, it is very easy to find the ratio of the number of lipid molecules in liquid-crystalline state ($N_{\mathrm{lc},T}$) to the total number of lipid molecules (N_b) in the MLVs bilayers:

$$\alpha_T = \frac{N_{\mathrm{lc},T}}{N_\mathrm{b}} . \tag{3}$$

In fact, f_T is connected to K_T, the partition coefficient of the spin-label between the lipid bilayers and water, by the equation

$$f_T = \frac{K_T(N_\mathrm{b}/N_\mathrm{w})}{1 + K_T(N_\mathrm{b}/N_\mathrm{w})} , \tag{4}$$

where N_w stands for the number of water molecules in the system, and where K_T can in turn be expressed as a weighted mean of the partition coefficients relative to the gel and liquid-crystalline phase [23]—say K_lc and K_g—as follows:

$$K_T = K_\mathrm{lc}\alpha_T + (1 - \alpha_T)K_\mathrm{g} . \tag{5}$$

From (5) and (4) one gets at once

$$\alpha_T = \frac{1 - f_\mathrm{lc}}{f_\mathrm{lc} - f_\mathrm{g}} \frac{f_T - f_\mathrm{g}}{1 - f_T} , \tag{6}$$

where f_lc and f_g are the values of the f_T parameter relative, respectively, to the

liquid-crystalline and gel phases, that coexist during the transition.

If one assumes that f_g practically coincides with the f_T value at the transition beginning, that is when all the lipid molecules are in the gel state, and likewise that f_{lc} coincides with the final value, when all the molecules are in liquid-crystalline state, then eq. (6) will furnish α_T through a simple evaluation of f_T. Therefore eq. (6) can be considered as describing the (thermal) evolution of gel → liquid-crystalline transitions.

More in general, since f_T behaviour in gel → gel transitions of $L_{\beta'} \rightarrow P_{\beta'}$ type is similar to the behaviour in gel → liquid-crystalline transitions (as fig. 4*a*) shows), we shall assume that the evolution of any transition between two consecutive states be describable by a parameter, obviously function of T, $\alpha_{ij,T}$ that—in strict analogy with eq. (3)—can be written as

$$\alpha_{ij,T} = \frac{N_{j,T}}{N_b}, \tag{7}$$

where indexes i, j respectively indicate the initial and final state. This parameter is

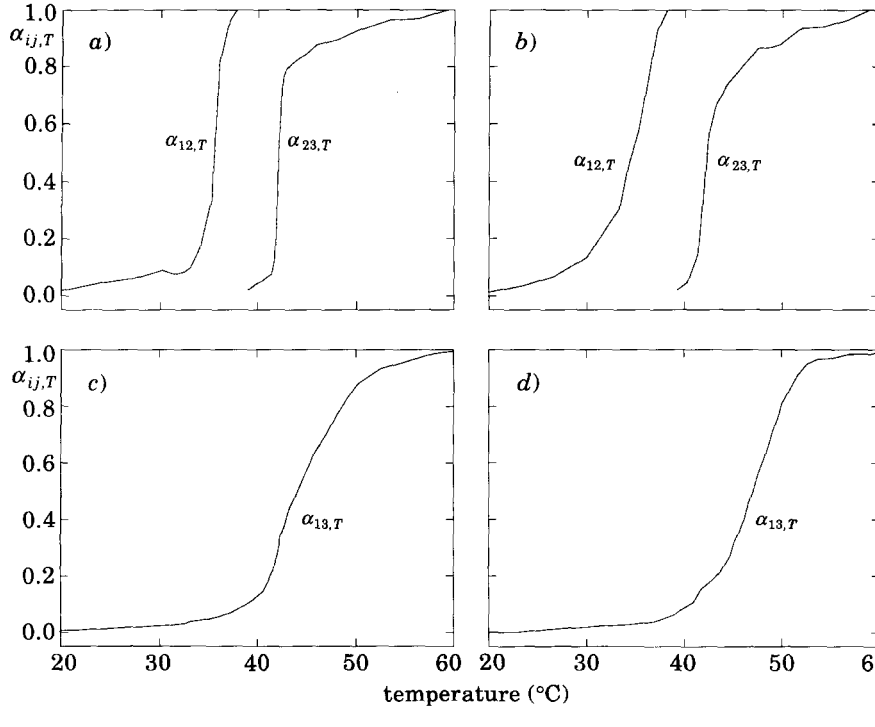

Fig. 5. – Evolution of the transitions with temperature, as described by $\alpha_{ij,T}$ parameter (see text). When two transitions are present, as in cases *a*) and *b*), the evolutions of both are reported. The MLVs compositions are those reported in fig. 2, respectively for: *a*) D_0; *b*) D_1; *c*) D_2; *d*) D_3.

connected to f_T by an equation analogous to (6):

$$\alpha_{ij,T} = \frac{1-f_j}{f_j-f_i}\,\frac{f_T-f_i}{1-f_T}, \tag{8}$$

where f_i and f_j stand respectively, for each transition, for the initial and final values of f_T, illustrated in fig. 4.

The thermal evolution of structural transitions of MLVs, both irradiated and unirradiated, monitored by the behaviour of the corresponding functions $\alpha_{ij,T}$ is shown in fig. 5. Figure 6 shows instead the temperature derivatives $\partial\alpha_{ij,T}/\partial T$, a more adequate representation, particularly for a comparison with DSC analysis results.

Specifically, for pure DPPC MLVs (see fig. 6*a*)), we can see that LT's evolution range is roughly 5 °C, MT's roughly 1 °C, which agrees with the ranges found by DSC technique, reproduced in fig. 3*a*). It may be observed that the maximum values of the transition rates, say with self-explanatory notation $(\partial\alpha_{LT}/\partial T)_{max}$ and $(\partial\alpha_{MT}/\partial T)_{max}$, stand in a 1 : 3 ratio, while the ratio of the corresponding calorimetric peaks heights, h_{LT} and h_{MT}, is ~ 1 : 19. It is easy to show that these values are actually mutually consistent. In fact, the heat flux associated with a transition evolution, assisted—as

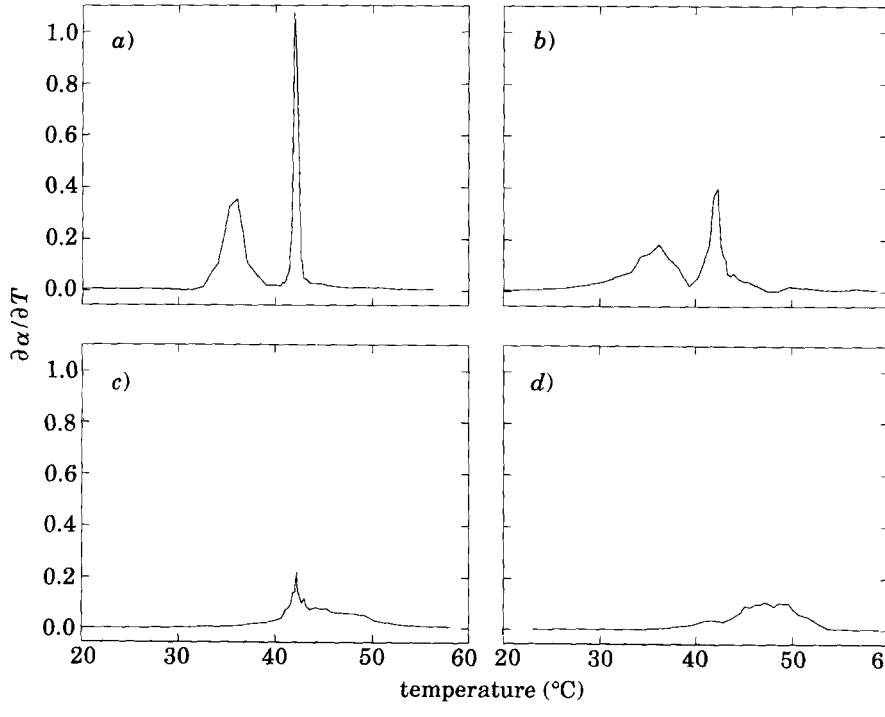

Fig. 6. – Rate of transition evolution with temperature $\partial\alpha_{ij,T}/\partial T$ (briefly indicated with $\partial\alpha/\partial T$) *vs.* temperature. The MLVs compositions are those reported in fig. 2, respectively for: *a*) D_0; *b*) D_1; *c*) D_2; *d*) D_3.

in the present case—by a temperature increase, is approximately given by

$$\frac{\partial Q}{\partial t} = \eta_{ij} \frac{\partial m_{ij}}{\partial t} = \eta_{ij} \frac{\partial T}{\partial t} \frac{\partial m_{ij}}{\partial T}, \tag{9}$$

where η_{ij} stands for the latent heat of the i-j transition; $\partial m_{ij}/\partial t$ for the time rate of transformation of lipid mass; $\partial T/\partial t$ for the scanning rate (actually constant); $\partial m_{ij}/\partial T$ for the rate of transformation of the lipid mass with temperature, that (see eq. (3)) should be proportional to $\partial \alpha_{ij}/\partial T$. Therefore, taking into account that the latent heats of MT and LT, η_{MT} and η_{LT}, stand in a ratio $\eta_{\mathrm{MT}}/\eta_{\mathrm{LT}} \cong 6$, one can precisely expect that

$$\frac{h_{\mathrm{MT}}}{h_{\mathrm{LT}}} = \frac{(\partial Q_{\mathrm{MT}}/\partial t)_{\max}}{(\partial Q_{\mathrm{LT}}/\partial t)_{\max}} \cong \frac{\eta_{\mathrm{MT}}}{\eta_{\mathrm{LT}}} = \frac{(\partial \alpha_{\mathrm{MT}}/\partial T)_{\max}}{(\partial \alpha_{\mathrm{LT}}/\partial T)_{\max}} \cong 18. \tag{10}$$

The mutual consistence of these results, one obtained from spin-label experiments and the other by DSC, that is by two entirely independent methods, can be considered to give remarkable support to the assumptions made above, concerning the evolution of structural thermotropic transitions.

For the irradiated MLVs, the behaviour *vs.* temperature of $\partial \alpha_{ij,T}/\partial T$ is given in fig. 6*b*), *c*) and *d*). As said above, the LT is visible only for low dose, though widened toward the low temperature, in full agreement with DSC results.

However, the most interesting results concern MT. This transition looks biphasic, meaning that, within its range, two regions are clearly distinguished. In the first region, that is between 40 and 43 °C, the evolution, initially rapid, slows down very quickly *vs.* the absorbed dose. In the second region, that approximately begins at 43 °C, and spreads progressively towards higher temperature, the evolution rate always remains very low. It is therefore clear that the MT peaks asymmetry, evidenced in fig. 3*b*), *c*), *d*), mirrors the difference of the evolution rates within the two mentioned regions.

It has been common belief that MT modifications in irradiated MLVs could altogether be related to LPC presence in the bilayers [6, 7]. Such assumption needs to be revised, in the light of the present results. In fact, the LPC concentration turns out to remain practically constant for a whole range of doses—as shown in fig. 2. It seems therefore strange that, in the same range, LPC might cause dramatic progressive reduction of the MT rate $(\partial \alpha_{\mathrm{MT}}/\partial T)_{\max}$ and also progressive MT widening. Let us observe moreover that LPC in water features a transition around 5 °C (fig. 7), much lower a temperature than that of MT occurrence. It seems thus quite unlikely that, when LPC is mixed with DPPC in the irradiated bilayers, it might cause MT widening precisely towards high temperature. This effect, on the contrary, can reasonably be attributed to FPA, that exhibits a transition around 60 °C (fig. 7). Actually, DSC of MLVs consisting of DPPC-FPA mixtures not only show MT to be widened towards high temperature, but also to be biphasic and with a slow evolution rate (fig. 7), like the MT of irradiated MLVs. This fact renders it very plausible that the reason why, in irradiated specimens, MT width (fig. 3 and 6) depends almost linearly on the dose, must be that precisely FPA's concentration grows linearly with the dose.

In the actuality, the molecular mechanisms through which FPA may cause the effects just described, are not fully clarified. Nevertheless, at least in the case of

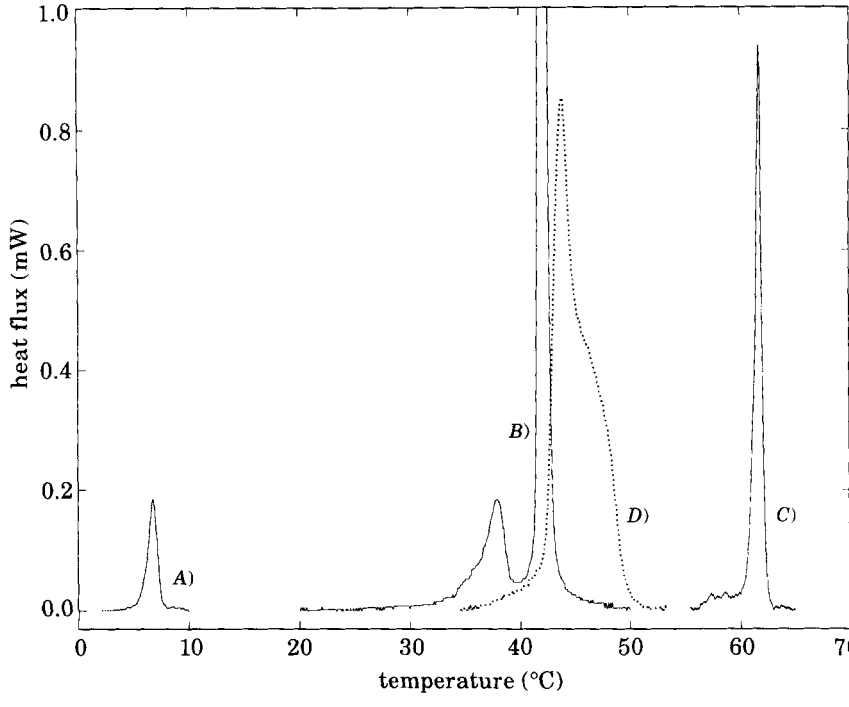

Fig. 7. – DSC curves showing the structural transitions for the systems with a single lipid component: *A*) LPC-water ($c_{LPC} = 1.0 \cdot 10^{-2}$, w/w), *B*) DPPC-water ($c_{DPPC} = 12.3 \cdot 10^{-2}$, w/w), *C*) FPA-water ($c_{FPA} = 0.6 \cdot 10^{-2}$, w/w); and with two lipid components: *D*) (FPA_xDPPC)-water ($c_{FPA_x DPPC} = 11.6 \cdot 10^{-2}$, w/w; molar ratio of FPA to DPPC, $x = 9.2 \cdot 10^{-2}$).

unirradiated bilayers, composed of mixtures of saturated DAPC with fatty acids, X-ray diffraction results suggest that the carboxyl group of the free fatty acid tends to be located mainly in the region between the carbonyl and the glycerol groups of the DAPC [34].

Therefore, as the steric hindrance of the FPA carboxyl group is much smaller than that caused by the DPPC head group, then the presence of FPA within the bilayers should entail a shortening of the average distance among acyl chains of the adjacent molecules, and a reinforcing of their interaction. This should in turn bring in a kind of stabilization of the gel structure, slowing down the evolution of the latter towards the liquid-crystalline structure.

The results obtained so far do not allow a sure understanding as to which role do play LPC interactions with DPPC and FPA, that are simultaneously present in irradiated bilayers. Moreover, LPC's influence on the initial transition temperature is not to be excluded. On the contrary, in irradiated specimens no significant GPC effect seems to exist.

* * *

We wish to thank Mr. S. Longoni for technical assistance. Financial support by the National Research Council (CNR) and by the Ministry of University and of Scientific and Technological Research (MURST) is acknowledged.

Acronym code.

The following code of often used acronyms may make the reading of this paper easier:

DAPC	1,2-diacyl-*sn*-glycero-3-phosphorylcholine,
DPPC	1,2-dipalmitoyl-*sn*-glycero-3-phosphorylcholine,
DSC	differential scanning calorimetry,
EPR	electron paramagnetic resonance,
FPA	free palmitic acid,
GPC	glycerophosphorylcholine,
LPC	P_1PC and/or P_2PC lysolecithins,
LT	«lower transition» (from $L_{\beta'}$ to $P_{\beta'}$ structure) in DPPC MLVs,
MT	«main transition» (from $P_{\beta'}$ to L_α structure) in DPPC MLVs,
MLVs	multi-lamellar vesicles of lipids in excess water,
NMR	nuclear magnetic resonance,
P_1PC	1-palmitoyl-*sn*-glycero-3-phosphorylcholine,
P_2PC	2-palmitoyl-*sn*-glycero-3-phosphorylcholine,
TEMPO	spin-label 2,2,6,6-tetramethylpiperidine-1-oxyl,
TLC	thin-layer chromatography.

REFERENCES

[1] K. A. FISHER and W. STOECKENIUS: in *Biophysics*, edited by W. HOPPE, W. LOHMANN, H. MARKL and H. ZIEGLER (Springer-Verlag, Berlin, Heidelberg, 1982) and references cited therein.
[2] W. D. STEIN: *Transport and Diffusion across Cell Membranes* (Academic, Orlando, Fla., 1986) and references cited therein.
[3] J. C. EDWARDS, D. CHAPMAN, W. A. CRAMP and M. B. YATVIN: *Prog. Biophys. Molec. Biol.*, **43**, 71 (1984) and references cited therein.
[4] G. STARK: *Biochim. Biophys. Acta*, **1071**, 103 (1991) and references cited therein.
[5] D. J. W. BARBER and J. K. THOMAS: *Radiat. Res.*, **74**, 51 (1978).
[6] F. IANZINI, L. GUIDONI, P. L. INDOVINA, V. VITI, G. ERRIU, S. ONNIS and P. RANDACCIO: *Radiat. Res.*, **98**, 154 (1984).
[7] G. ALBERTINI, E. FANELLI, L. GUIDONI, F. IANZINI, P. MARIANI, M. MASELLA, F. RUSTICHELLI and V. VITI: *Int. J. Radiat. Biol.*, **52**, 145 (1987).
[8] M. CASU, A. LAI, G. ERRIU, S. ONNIS and N. ZUCCA: *Magn. Reson. Chem.*, **30**, 408 (1992).
[9] G. ERRIU, M. LADU and G. MELEDDU: *Biophys. J.*, **35**, 799 (1981).
[10] G. ERRIU, M. LADU, G. MELEDDU and S. ONNIS: *Lett. Nuovo Cimento*, **34**, 215 (1982).
[11] G. ERRIU, S. ONNIS, P. RANDACCIO, C. GIORI and G. SCHIANCHI: *Lett. Nuovo Cimento*, **44**, 51 (1985).
[12] M. CAFFREY: *Nucl. Instrum. Methods Phys. Res.*, **222**, 329 (1984).
[13] G. ALBERTINI, E. FANELLI, L. GUIDONI, F. IANZINI, P. MARIANI and F. RUSTICHELLI: *Int. J. Radiat. Biol.*, **48**, 785 (1985).
[14] D. F. REGULLA and U. DEFFNER: *Int. J. Appl. Radiat. Isot.*, **33**, 1101 (1982).
[15] A. BARTOLOTTA, P. L. INDOVINA, S. ONORI and A. ROSATI: *Radiat. Protec. Dosimetry*, **9**, 277 (1984).
[16] D. CHAPMAN, R. M. WILLIAMS and B. D. LADBROOKE: *Chem. Phys. Lipids*, **1**, 445 (1967).
[17] A. TARDIEU, V. LUZZATI and F. C. REMAN: *J. Mol. Biol.*, **75**, 711 (1973).
[18] M. J. JANIAK, D. M. SMALL and G. G. SHIPLEY: *Biochemistry*, **15**, 4575 (1976).

[19] O. H. GRIFFITH and P. C. JOST: in *Spin Labeling Theory and Applications*, edited by L. J. BERLINER, Vol. 1 (Academic, New York, N.Y., 1976) and references cited therein.
[20] E. SACKMANN: in *Biophysics*, edited by W. HOPPE, W. LOHMANN, H. MARKL and H. ZIEGLER (Springer-Verlag, Berlin, Heidelberg, 1982) and references cited therein.
[21] G. M. K. HUMPHRIES and H. M. MCCONNELL: in *Methods of Experimental Physics: Biophysics*, edited by G. EHRENSTEIN and H. LECAR, Vol. 20 (Academic, New York, N.Y., 1982) and references cited therein.
[22] G. ERRIU, S. ONNIS, N. ZUCCA, C. GIORI and G. SCHIANCHI: *Nuovo Cimento D*, **10**, 663 (1988).
[23] E. J. SHIMSHICK and H. M. MCCONNELL: *Biochemistry*, **12**, 2351 (1973).
[24] C. W. M. GRANT, S. H. W. WU and H. M. MCCONNELL: *Biochim. Biophys. Acta*, **363**, 151 (1974).
[25] S. H. W. WU and H. M. MCCONNELL: *Biochemistry*, **14**, 847 (1974).
[26] H. M. MCCONNELL: in *Spin Labeling Theory and Applications*, edited by L. J. BERLINER, Vol. 1 (Academic, New York, N.Y., 1976).
[27] S. MABREY and J. M. STURTEVANT: *Proc. Natl. Acad. Sci. USA*, **73**, 3862 (1976).
[28] A. G. LEE: *Biochim. Biophys. Acta*, **472**, 237 (1977) and references cited therein.
[29] J. F. NAGLE: *Proc. Natl. Acad. Sci. USA*, **70**, 3443 (1973).
[30] M. CAFFREY, G. FANGER, R. L. MAGIN and J. ZHANG: *Biophys. J.*, **58**, 677 (1990).
[31] A. R. UBBELOHDE: *Melting and Crystal Structure* (Clarendon, Oxford, 1965).
[32] C. W. M. GRANT and H. M. MCCONNELL: *Proc. Natl. Acad. Sci. USA*, **71**, 4653 (1974).
[33] P. H. J. T. VERVERGAERT, A. J. VERKLEIJ, P. F. ELBERS and L. L. M. VAN DEENEN: *Biochim. Biophys. Acta*, **311**, 320 (1973).
[34] F. PODO and J. K. BLASIE: *Biochim. Biophys. Acta*, **419**, 1 (1976).